ELSEVIER

Biophysical Chemistry 113 (2005) 137–144

Biophysical Chemistry

www.elsevier.com/locate/bpc

HEW lysozyme salting by high-concentration NaCl solutions followed by titration calorimetry

Jarosław Poznański*, Małgorzata Wszelaka-Rylik, Wojciech Zielenkiewicz*

Institute of Physical Chemistry, Polish Academy of Sciences, Kasprzaka 44/52, 01-224 Warsaw, Poland

Accepted 31 August 2004
Available online 29 September 2004

Abstract

Concentration dependence of NaCl salting of 0–1.5 mM lysozyme solution in 0.1 M sodium acetate buffer, pH 4.25, was investigated for NaCl concentration varying up to 0.9 M. Calorimetric experiments demonstrated that depending on the salt concentration the estimated number of the binding sites on the lysozyme surface varied in the range of 5 up to 13, and the increase of salt concentration caused the decrease of the number of accessible sites. The small, but significant, local maximum centered at 0.63 M NaCl concentration indicated the specific salting-out of the lysozyme accompanied by binding of ~2–3 chloride anions. Generalized McMillan and Mayer's approach reduced to the third-order virial coefficients demonstrates the domination of lysozyme aggregation upon salt addition (a_{21}–h_{xxy}) and salt organization on the lysozyme surface (a_{12}–h_{xyy}) processes.

Keywords: Lysozyme; Salt binding; Titration calorimetry; Virial coefficients

1. Introduction

Hen-egg white lysozyme has been exhaustively used the past decade as a model for elucidating the mechanism of protein crystal growth. Protein nucleation kinetics was interpreted in the terms of the protein supersaturated solution nonideality [1,2] and allowed identification of fractallike aggregates as probable morphological instabilities during crystal growth [3,4]. Using time-resolved DLS, Tanaka et al. [5,6], Eberlis et al. [7] and Georgalis et al. [8] confirmed the coexistence of oligomers and clusters in supersaturated lysozyme solutions. At the same time, Bishop et al. [9] published DLS measurements on supersaturated lysozyme solutions, emphasizing the effect of intermolecular interactions. Time-resolved small-angle neutron scattering studies of supersaturated lysozyme solutions shoved that the detection of larger clusters is very difficult using either X-ray or neutron wavelengths [10,11]. Recently, the lysozyme aggregation process was followed by NMR techniques [12,13].

George and Wilson [14] pointed to the idea of second virial coefficient slots, which allows the prediction optimal crystallization conditions from SLS measurements in dilute protein solutions. The probability for a protein to crystallize is higher when the second virial coefficient is negative. The concept of second virial coefficient slots inspired also theoretical predictions [15,16] using Baxter's [17] "stickiness" coefficient as a function of the protein volume fraction.

The most dominant factors influencing kinetics of lysozyme nucleation are salt composition and both protein and salt concentrations [18]. The high resolution crystallographic structures of hen-egg white lysozyme in the triclinic [19], monoclinic [20], orthotombic [21] and tetragonal [22–25] crystal forms demonstrate the existence of up to 8 weakly bound chloride anions [24]. The lysozyme was proved to bind 21–23 chloride anions per

* Corresponding authors. Tel.: +48 22 632 43 89; fax: +48 22 632 52 76.
E-mail addresses: jarek@ichf.edu.pl (J. Poznański), zivf@ichf.edu.pl (W. Zielenkiewicz).

0301-4622/$ - see front matter © 2004 Elsevier B.V. All rights reserved.
doi:10.1016/j.bpc.2004.08.007

molecule in the saturated solution in a sodium acetate/NaCl buffer [26]. Recently, systematic investigations on the chloride anion occupancy in the protein crystals demonstrated that halide anions exhibited ability to relative nonspecific partial substitution of water molecules within the ordered protein solvation shell [27]. In order to enrich knowledge of the salting of the lysozyme, we have decided to perform a systematic study of thermodynamic properties of the binding of a chloride anion to the lysozyme in unsaturated solution by the use of an isothermal titration microcalorimeter ITC MicroCal.

2. Experimental

Hen egg lysozyme was purchased from Fluka, dissolved in Millipore water, dialyzed against Millipore water to remove salts, and lyophilized. Prior the measurements the lysozyme powder was dissolved in 0.1 M acetic/NaOH buffer (pH 4.25), filtered through 0.22-μm syringe filter (Roth, Germany) and degassed. The pH value of the buffer as well as of the lysozyme stock and NaCl-buffered solutions were adjusted independently (±0.05 pH) using a Mettler Toledo pH-meter (MP 220). The protein concentration was determined by UV absorption spectrum, assuming the extinction coefficient ε_{280}=38 220 $M^{-1}\cdot cm^{-1}$. Analytical-grade sodium chloride was purchased from Merck.

The calorimetric experiments were performed with the use of a titration ITC Omega MicroCal microcalorimeter. The 7 mM buffered lysozyme solution was injected in small volumes of 15 μl, in a series of 20 controlled pulses to the final concentration of 1.3 mM in a sample cell of the volume 1.3611 ml. The experiments were made in the conditions where the sample cell initially contained the adequate NaCl solution in 0.1 M sodium acetate buffer, whereas the reference cell was filled with the pure buffer. NaCl concentration in the sample cell varied in the range of 0.3–0.9 M.

3. Numerical methods

The experimental data obtained from the calorimetric titration were analyzed based on the model of a single set of identical sites [ITC Tutorial Guide]. The association equilibrium and mass balance for the ligand could be expressed in the form:

$$K = \frac{\Theta}{(1-\Theta)[X]}$$

$$X_t = [X] + n\Theta M_t \tag{1}$$

where K is the binding constant, $[X]$ is concentration of free ligand and Θ is a fraction of sites occupied by ligand, X_t is a total concentration of the ligand, M_t is a total concentration of the protein and n is a number of binding sites. Resolving the Eq. (1) against the fraction of sites occupied by ligand one could estimate the total heat effect of the binding:

$$Q = n\Theta M_t \Delta H V_0 = \frac{nM_t\Delta H V_0}{2}\left[1 + \frac{X_t}{nM_t} + \frac{1}{nKM_t} - \sqrt{\left(1 + \frac{X_t}{nM_t} + \frac{1}{nKM_t}\right)^2 - \frac{4X_t}{nM_t}}\right] \tag{2}$$

where ΔH is the molar heat of a ligand binding and V_0 is an active cell volume.

The theoretical value of Q could be calculated for any state of the solution described by protein, M_t, and ligand, X_t, concentrations, using assumed parameterization describing ligand–macromolecule interaction: K, ΔH and n. The three latter parameters should be optimized using experimental titration calorimetric data. The only important customization is the correction of total experimental heat effect involved in a series of n injections, $Q^{exp}(n)$, for the volumes displaced upon injection [13].

$$Q^{exp}(n) = \sum_{k=1}^{n} \frac{\Delta Q^{exp}(k)\left(1 - \frac{dV}{2V_0}\right)^{n-k}}{\left(1 + \frac{dV}{2V_0}\right)^{n-k+1}} \tag{3}$$

where $\Delta Q^{exp}(k)$ is the heat released upon the k-th injection of the volume dV to the cell of the volume V_0.

The process of fitting model (Eq. (2)) to the experimental data, $Q^{exp}(i)$, (Eq. (3)) was carried out with the use of implementation of Marquardt–Levenberg nonlinear least-squares algorithm [28] from gnuplot [29].

The standard McMillan and Mayer's approach [30] was generalized according to the ideas of Franks et al. [31] and reduced to the triplet coefficients, as presented in the simplified form:

$$\tilde{Q}(n) = \sum_{\substack{i+j<4 \\ i,j>0}} a_{ij}(M_{t,n})^j (X_{t,n})^i \tag{4}$$

where $\tilde{Q}(n)$ is the total heat effect involved in the series of n succeeding injections, $X_{t,n}$ and $M_{t,n}$ are the salt and lysozyme concentrations in the sample cell after n–th injection. The a_{ij} is the shortened notation of the $h_{\underbrace{x,\ldots,x}_{i\ times}\,\underbrace{y,\ldots,y}_{j\ times}}$ coefficient.

Analogously to the analysis of binding sites-based model, $Q^{exp}(n)$ was corrected for the volumes displaced upon injections. The parameters a_{ij} were optimized to minimize the deviations between the estimated enthalpy change upon binding, $\tilde{Q}(n)$, (Eq. (4)) and the experimentally

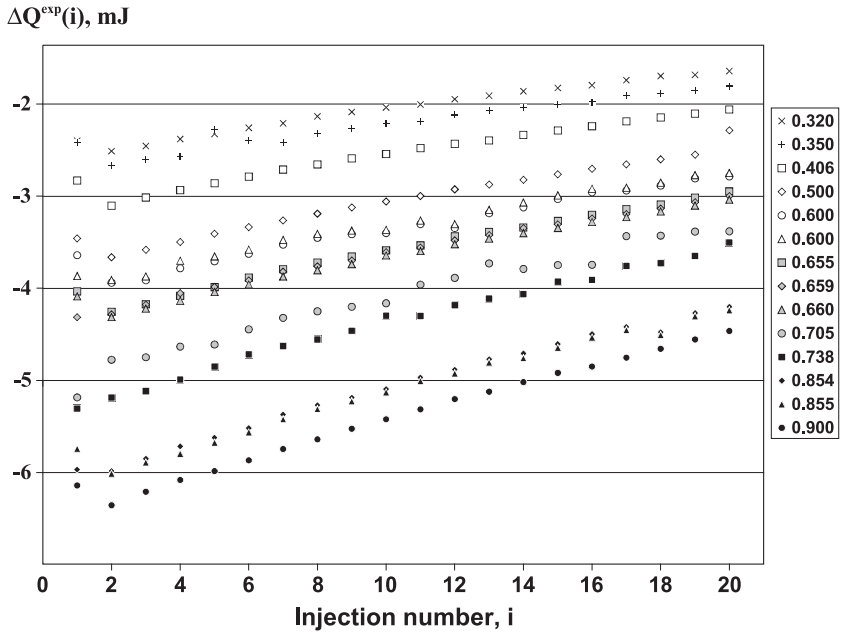

Fig. 1. The titration experiment represented as a function of injection number. The markers follows the experimentally observed heat released upon single injection to the various NaCl concentration in the sample cell (0.3–0.9 M). Every experimental data arise from injection of 15 μL of 7 mM lysozyme solution to the sample cell filled initially with a buffered NaCl in the concentration of 0.3–0.9 M.

derived $Q^{\exp}(n)$ (Eq. (3)). The models' quality was analyzed in the terms of χ^2 test [32]. The successive reductions of the number of virial coefficients used in the model were made based on Student's t-statistics [32]. The coefficients with the lowest t-statistics were successively removed from the analysis.

4. Results and discussion

4.1. Calorimetric titration data

Experimental data were obtained for 14 series of experiments, in which the lysozyme concentration in the syringe

Table 1
The integrated heat effects of each of 20 successive injections, ΔQ^{exp} (i), obtained for 14 series of lysozyme injections to a different NaCl solutions, m_y

Exp.	0	1	2	3	4	5	6	7	8	9	10	11	12	13	14
$m_y/(M)$	0.000	0.320	0.350	0.406	0.500	0.600	0.600	0.655	0.659	0.660	0.705	0.738	0.854	0.855	0.900
Injection no. (i)	$-\Delta Q^{exp}$ $(i)/mJ$														
1	−0.75	2.36	2.38	2.80	3.42	3.83	3.61	4.00	4.28	4.05	5.15	5.27	5.93	5.71	6.11
2	−0.98	2.48	2.64	3.07	3.63	3.88	3.91	4.22	4.25	4.28	4.74	5.15	5.95	5.98	6.32
3	−0.94	2.42	2.57	2.98	3.55	3.84	3.88	4.14	4.14	4.19	4.71	5.08	5.82	5.86	6.17
4	−0.89	2.34	2.53	2.90	3.46	3.67	3.75	4.05	4.02	4.10	4.60	4.96	5.68	5.76	6.05
5	−0.85	2.29	2.24	2.82	3.37	3.62	3.67	3.95	3.95	4.00	4.58	4.82	5.59	5.64	5.95
6	−0.82	2.22	2.36	2.75	3.30	3.55	3.59	3.85	3.88	3.92	4.41	4.68	5.49	5.53	5.83
7	−0.79	2.17	2.38	2.68	3.23	3.44	3.49	3.76	3.79	3.84	4.29	4.59	5.34	5.39	5.71
8	−0.75	2.10	2.29	2.62	3.16	3.38	3.42	3.69	3.73	3.77	4.22	4.52	5.24	5.28	5.61
9	−0.73	2.05	2.23	2.56	3.09	3.34	3.38	3.62	3.66	3.70	4.17	4.43	5.15	5.19	5.49
10	−0.70	2.00	2.18	2.51	3.02	3.33	3.37	3.55	3.57	3.61	4.13	4.26	5.06	5.10	5.39
11	−0.68	1.97	2.16	2.44	2.96	3.23	3.27	3.50	3.52	3.56	3.93	4.27	4.93	4.97	5.28
12	−0.66	1.91	2.08	2.40	2.89	3.27	3.31	3.40	3.45	3.49	3.85	4.15	4.85	4.89	5.17
13	−0.64	1.87	2.03	2.36	2.84	3.11	3.15	3.35	3.39	3.43	3.70	4.08	4.73	4.77	5.09
14	−0.63	1.83	2.00	2.30	2.79	3.03	3.09	3.31	3.31	3.37	3.75	4.03	4.67	4.72	4.98
15	−0.61	1.79	1.97	2.25	2.73	2.96	3.00	3.23	3.27	3.31	3.71	3.89	4.57	4.61	4.88
16	−0.59	1.76	1.94	2.21	2.67	2.89	2.92	3.17	3.21	3.25	3.71	3.87	4.46	4.50	4.82
17	−0.57	1.70	1.88	2.15	2.62	2.87	2.90	3.11	3.16	3.19	3.40	3.72	4.39	4.42	4.72
18	−0.56	1.66	1.85	2.11	2.57	2.82	2.85	3.06	3.10	3.13	3.39	3.69	4.44	4.47	4.62
19	−0.54	1.65	1.82	2.07	2.51	2.74	2.77	2.98	3.03	3.07	3.35	3.61	4.23	4.27	4.52
20	−0.75	1.61	1.77	2.02	2.46	2.71	2.75	2.91	2.97	3.00	3.35	3.47	4.17	4.20	4.43

The experimental values were corrected for the heat effect of injection of the pure buffer to a sample cell filled by the identical salt solution and for the heat effect of injection of the identical 7 mM lysozyme solution to a sample cell filled by pure buffer (experiment 0).

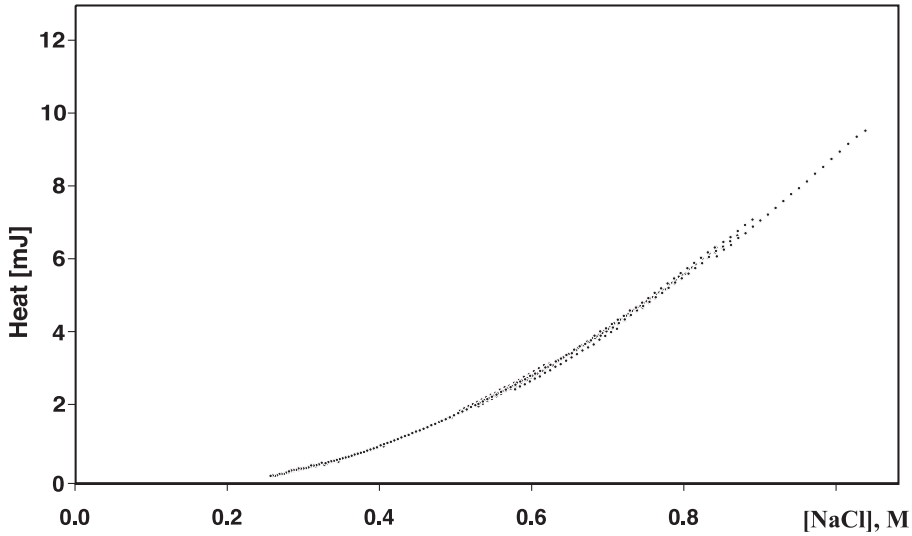

Fig. 2. The NaCl dilution heat released upon injection 15 μL of buffer to the sample cell of the volume 1.36 mL filled with the buffered salt solution. The experimental data (· · ·) were obtained from 14 independent experiments. The small deviations from the uniform continuous curve are resulting from biases in salt concentration determination.

was practically identical (7 mM), whereas the salt concentrations in the sample cell varied from 0.3 to 0.9 M (Fig. 1). Each experiment consisted of 20 succeeding injections. The integrated heats are demonstrated as a function of injection number in Table 1, where m_y is the initial concentration of NaCl in the sample cell. The integrated heat effects of each injection were corrected for both the corresponding integrated heat effects of lysozyme injection to the pure buffer and salt dilution by pure buffer injection. The experimental error of the individual experiment was assumed as 2% of the integrated heat effect arising from the corresponding injection. Because all of the experiments were performed independently, the experimental bias of the heat effect corrected for dilutions was estimated as the square root of the sum of the squared errors of arising from the three participating heat effects.

4.2. Heat effect of lysozyme dilution upon injection

Uniform pattern of the concentration dependence of the lysozyme dilution is consistent with previous experimental data [33]. The interactions between lysozyme–lysozyme pairs are thermochemically favorable. Attraction forces, which result in the observed negative h_{xx} values dominates over the effect of dehydration. The lysozyme contains in their molecules functional groups that can interact by means of hydrogen bond formation and dipole–dipole interactions. The presence of charged ionic groups also enables ion–dipole interactions. These interactions seem to be relatively strong due to the weak hydration of the lysozyme molecules.

4.3. Heat effect of salt dilution upon buffer injection

The reference experiments made in parallel to the lysozyme to salt injection demonstrated the self-consistent pattern of the salt dilution heat effect. Upon a series of buffer injections the NaCl solution the salt concentration in the sample cell was changing so significantly that the individual experimental curves overlapped, as it is presented in Fig. 2. The overlapping of the individual experiments demonstrates the quality of the data. The small disagreements between the experimental series were the consequence of biases in the setting the initial salt concentration.

4.4. Total heat effect of lysozyme injection to the salt solution

Experimental data of the 14 series of lysozyme injections to the salt solution as well as pure lysozyme dilution effect are collected in Table 1. The total heat effect of the series of 20 succeeding lysozyme injections could be represented as a monotonic function of the salt concentration, the increase of the NaCl concentration enlarges the negative value of the total heat effect. Despite the general tendency, the systematic deviations are observed for the salt concentration lying in the range of 0.5–0.7M. These deviations could be easily attributed to the specific salting-out process of lysozyme, which was found the most efficient for the 0.63 NaCl solution [26]. The quality of the data could be judged in Fig. 3. In parallel, the estimated effect of the lysozyme salting-out defined as the deviation from the general second-order trend is presented. For the eye guide, the Gaussian-shaped curve centered at 0.63 M NaCl concentration follows the experimentally observed deviation from general second order polynomial trend.

4.5. Virial coefficients

The global analysis of the experimental data of the heat effect was initially performed in the terms of virial

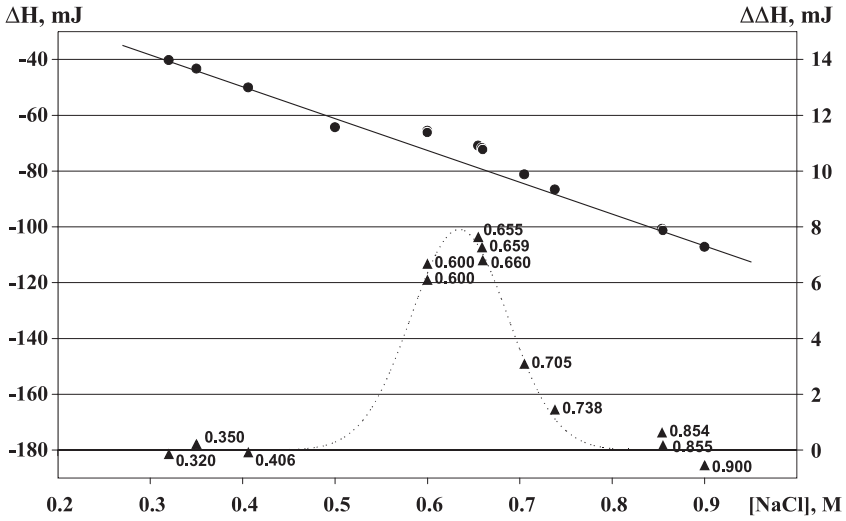

Fig. 3. Total heat effect, ΔH, of the series of 20 injections of 7 mM lysozyme solution expressed as a function of salt concentration in the sample cell (•, left axis). In the bottom, the deviation, ΔΔH, of ΔH from the second-order approximation (▲, right axis). Each data point corresponds to independent titration experiment. The quadratic approximation (- - -) and Gaussian type curve centered at 0.63 M NaCl (—) are presented as eye guides to follow the general trends in concentration dependence of the heat effect.

pairwise and triplet coefficients [31]. The model was subsequently reduced by removing the less-significant, in the terms of Student's *t*-value, parameter. The general formula of the equation used was initially in the form Eq. (4), where the total heat effect, $\tilde{Q}$, arising from mixing solutions of an adequate concentrations of lysozyme and NaCl was compared with the experimental data corrected for the displaced volumes according to the Eq. (3). The documentation of a series of optimization procedures is presented in Table 2.

Calculations started from the maximal set of 10 coefficients proved that some of them were statistically insignificant. The agreement of a given model with the experimental data was verified by χ^2 values. In every cycle of the analysis, the coefficient with the lowest Student's *t*-value, which is a measure of the coefficient's significance, was systematically removed. The optimal set of parameters was chosen as that which reduction caused the significant increase of the χ^2 value. This procedure led to the reduced set of parameters showing almost unchanged χ^2 values.

The simplest acceptable model is a three-parameter one, and the succeeding reduction of the number of model parameters led to the significant increase of the χ^2 value. The most important parameters found are a_{12} and a_{21} corresponding to three-body interactions, which could be interpreted as salt-induced lysozyme aggregation (a_{21}) and salt organization on the lysozyme surface (a_{12}). The a_{10} (h_x) parameter arises from the nonideal correction for the lysozyme dilution effect. Taking into account that there are some controversies about the usage of so large set of parameters [34], the additional series of modeling, started from the second order coefficients, was performed.

All the parameters of the selected models are summarized in the Table 2. The final, three-parameter model (a_{10}, a_{21}, a_{12}) is presented in Fig. 4.

Table 2
The virial coefficients determined for the salting of lysozyme solutions according to the Eq. (4) with the correction for the displaced volume presented in Eq. (3)

Parameter	8		4		3		2		6		2		1	
	Value	*t*-Stat	Value	*t*-Stat	Value	*t*-Stat	Value	*t*-Stat	Value	*t*-Stat	Value	*t*-Stat	Value	*t*-Stat
$a_{00}/(10^{-4}$ J)	4(3)	1.1							−30(4)	8.0				
$a_{10}/(\mathrm{J\ M^{-1}})$	−25(2)	12.8	−26(0.4)	72.0	−23(0.2)	74.9	−25(0.3)	88.6	−7(7)	0.9				
$a_{01}/(10^{-3}\ \mathrm{J\ M^{-1}})$	−1(1)	0.8							11(1)	8.4				
$a_{02}/(10^{-3}\ \mathrm{J\ M^{-2}})$	1(1)	0.7							−9(1)	7.9				
$a_{11}/(\mathrm{J\ M^{-2}})$	−1(6)	0.2							−91(1)	87.4	−91(0.5)	190	−97(0.4)	256
$a_{20}/(10^3\ \mathrm{J\ M^{-2}})$	6(1)	5.4	6(1)	9.4					−35(5)	7.8	−42(3)	15.3		
$a_{12}/(\mathrm{J\ M^{-3}})$	−69(6)	12.4	−71(1)	67.1	−79(1)	111.3	−83(1)	86.4						
$a_{21}/(10^3\ \mathrm{J\ M^{-3}})$	−21(2)	9.0	−21(1)	16.2	−10(0.5)	17.8								
χ^2	122		122		162		343		200		262		483	
χ^2/df	0.45		0.45		0.58		1.23		0.73		0.94		1.73	

Different sets of parameters were used. The reduction of the number of parameters influences the χ^2 value.

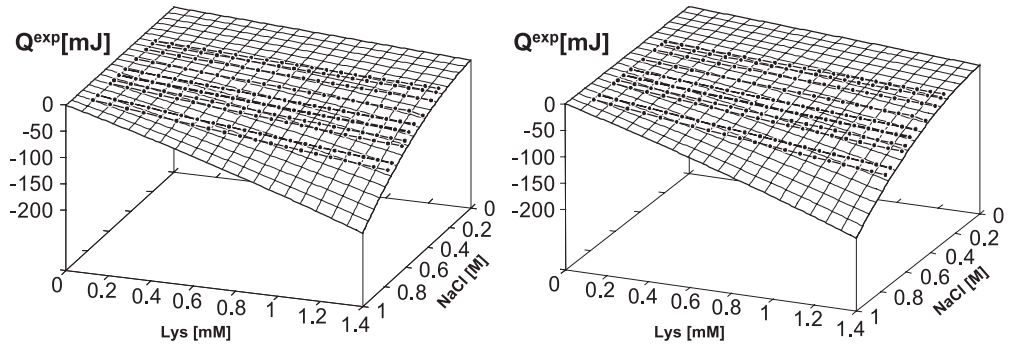

Fig. 4. The titration experiments represented as a function of lysozyme and salt concentrations. The circles correspond to the experimental data, thick lines represent successive salt injections in one experiment, surface represents the fitted model of 3 virial coefficients according to Eq. (4) with the correction for displaced volume through Eq. (3). The parameters used in the model mimic: salt induced lysozyme aggregation (a_{21}), salt organization on the lysozyme surface (a_{12}) and nonideal correction for the lysozyme dilution (a_{10}).

Additionally the global screening of the regression parameters was done. All the possible combinations of three, $\binom{8}{3}$ -56 combinations, and two, $\binom{8}{2}$ -28 combinations, parameter sets were analyzed in the terms of the χ^2 values of the optimized model. The best three-parameter model was found to base on the a_{10}, a_{21} and a_{12} parameters, while the best two-parameter one based on a_{11} and a_{20} ones. These results are in the perfect agreement with the rationalized parameter reduction procedure, as presented in Table 2. The reliability of the two proposed reduced models seems debatable. But the generally accepted trend to restriction the models to the second-order parameters drove to the set of different two-body parameterizations, and each of them is worse than the proposed three-parameter model based on a third-order $a_{21,}$ a_{12} and a_{10} parameters. On the other hand, the salt-induced protein aggregation process is evident for the analyzed system, and thus every model, a priori restricted to the two-body interaction (e.g., neglecting Lysozyme–Lysozyme–Cl^- and Lysozyme–Cl^-Cl^-), cannot properly describe lysozyme aggregation upon salt binding or simultaneous anion binding on the lysozyme surface. Generally, there is a strong need for the standardization of the decomposition the heat phenomena using virial coefficient approach. In real systems, the experimental boundaries, especially the range of components concentration, favor or disfavor a different sets of parameters. One must also take into account that variations in component concentrations may dramatically change the dominant association equilibrium, and in consequence, switch the screening procedure to the different set of parameters.

4.6. Model of n independent weakly binding sites

The titration curve was assumed in the form $Q(n_i, K, \Delta H,$ [Lys], [NaCl]), according to Eq. (2). Basing on the experience with the detailed analysis of the calorimetric data of lysozyme–NaCl interaction [35], the global analysis of the 14 experiments was performed simultaneously. The two uniform parameters: binding constant, K, and heat of binding, ΔH, were introduced to the model, while the number of binding sites, n_i, varied in the individual series as a function of initial salt concentration in the sample cell. The optimization of the Eq. (2) using global analysis of the 14 series of experiments consisting 20 succeeding lysozyme injections to a sample cell filled with a NaCl solution enable to estimate the general model parameters K=40(10) M^{-1} and ΔH=−80(23) kJ/mol. All the parameters of the model are strongly correlated (~0.9), which is resulting in relatively large errors of the estimated values. The standard deviations of the estimated individual n_i values exceeds 20%, which precluded any statistical analysis of the concentration dependence. To overcome this problem, the alternative approach was proposed to reduce the uncertainty of estimated n_i values. The biases of the estimated n_i parameters could be attributed to the two different error sources. The first one, dominating, is arising from the strong uncertainty in the determination of K and ΔH values, which are strongly correlated with all the n_i parameters. The other one is corresponding to the biases of the relative ratios of n_i values, which are mostly uncorrelated. If the analysis is focused on the general trends in NaCl induced changes of the n_i values, and no information about the absolute n_i values is required, the two model parameters, K and ΔH, assumed universal for all experimental series, might be kept fixed upon optimization procedure. In consequence, the relative biases of the estimated n_i parameters are reduced by the formal separation from the biases correlated with uncertainty of K and ΔH parameters. One must take into account that the proposed formal approach increased only the precision of the estimation of general trend observed for $n(c)$ relation. The absolute values of the individual n_i parameters are of course much more biased, as were determined initially (~20%). The trend in salt concentration dependence of the number on Cl^- binding sites on the lysozyme surface estimated in the proposed approach is presented in Fig. 5. The numeric data were obtained for the model of n independent binding sites (Eq. (2)), while the values of K and ΔH were constrained, K=40 M^{-1} and ΔH=−80 kJ/mol, respectively.

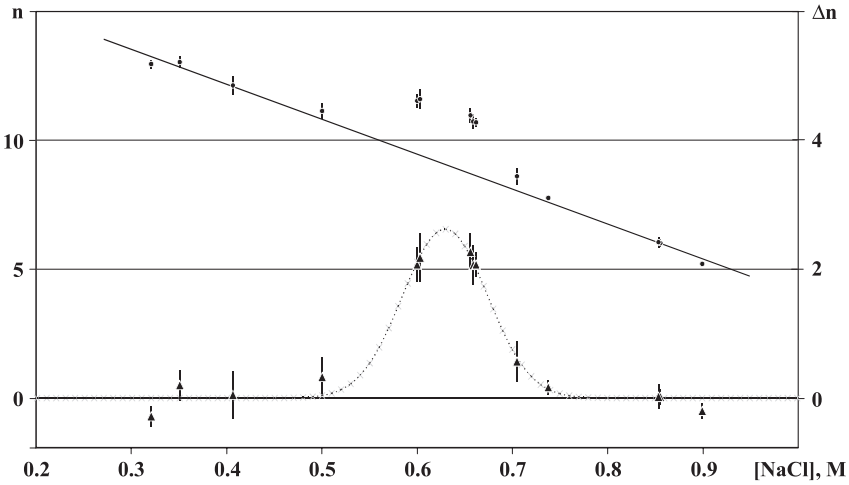

Fig. 5. The estimated number, n, of weakly binding centers on the lysozyme surface as a function of the NaCl concentration. (•) Number of binding sites on the lysozyme surface estimated basing on the model of the n independent binding sites (Eq. (2)) with the binding constant, K, constrained at 40 M^{-1}. (▲) Follows the deviation, Δn, from an idealized linear trend. This relation exhibits maximum localized at ~0.63 M NaCl, which indicates lysozyme salting-out by 2–3 Cl^- anions. The vertical bars mark the part of bias related directly with the analyzed trend in $n(c)$ dependence.

It is evident that the number of binding sites is decreasing almost linearly as the NaCl concentration is increased, demonstrating the effect of the universal process of the protein aggregation induced by the electrostatic screening phenomena. Despite the general monotonic trend, the significant deviations are observed in the range 0.5–0.7 M of NaCl concentration. The separation from the estimated linear trend, Δn, significantly exceeds the estimated reduced bias participating in the $n(c)$ trend determination. Thus, the NaCl specific salting-out process could be undoubtfully attributed to the changes of salt concentration. At 0.63 M NaCl, the limited uptake of 2–3 chloride anions undergoes against the general trend of the systematic decrease of the number of binding sites on the lysozyme surface.

5. Discussion

The proposed method of the simultaneous fitting of a single model, to the all series of titration experiments, drove as to estimate K and set of n_i values even for such a weakly binding system. The formal separation from the binding constant-related biases enabled to show the statistical significance of the observed salt related changes of the number of binding sites. The experiments covered the range of the relatively large range of salt concentration, while the lysozyme concentration was relatively small (0.1–1.4 mM). Thus, the obtained data could not be directly referred to our previously reported experiments [35], in which NaCl solution was injected to the lysozyme solution. Despite that, using direct extrapolation of the number of binding sites as a function of salt concentration to the 100 mM NaCl, one could, according to the relation presented in Fig. 5, estimate the number of binding sites for 1.5 mM lysozyme solution in 0.1 M NaCl solution for 17, which generally agrees with the value of ~35 estimated previously (cf Fig. 5 in Ref. [35]). Both these numbers are close to the value of 17 obtained with the aid of SPQ fluorescence measurement [26]. Analogously, the individual binding constant, actually estimated for 40(10) M^{-1}, is in the same order of value, as 2.7(8) M^{-1} determined previously, and agrees with experimentally observed partial occupation of halide anions observed for the short cryo-soaking of protein crystals [27].

Global analysis of the virial coefficients permitted to choose the most dominant, which were the a_{12}, and a_{21}, both corresponding to the three-body interaction. The a_{21} parameter could be interpreted as the lysozyme aggregation upon salt binding, while a_{12} corresponds to a kind of salt organization on the lysozyme surface. Both the parameter values could be also expressed as the virial coefficients normalized for the active cell volume and solute density and equal $h_{xxy}=1/3\ a_{21}=(-3.4\pm0.2)$ kJ kg^2 mol^{-3}, $h_{xyy}=1/3\ a_{12}=(-26\pm1)$ J kg^2 mol^{-3} kJ kg^2 mol^{-3}, respectively.

The most important observation arising from presented data was the statistically significant evidence of the specific process of salting lysozyme by NaCl. The optimal salt concentration was estimated as 0.63 M using three independent methods: analysis of the total heat released upon a whole series of lysozyme injection (Fig. 3) and analysis of the concentration dependence of the number of binding sites on the lysozyme surface (Fig. 5). Both presented approaches demonstrate the identical relation of the salt concentration, in agreement with tendencies observed by SPQ titration analysis [26]. The obtained value, 0.63 M NaCl, is in perfect agreement with a detailed analysis of the fractal dimension of salt-induced lysozyme aggregates based on both dynamic light scattering technique [8,36,37] and SPQ experiments [26]. Thus, the presented work demonstrates possibility of the usage of micro-calorimetry as the independent method for determination the optimal salt composition in protein crystallization.

Acknowledgement

We gratefully acknowledge the financial support from KBN within the grant No. 7T09A10621.

References

[1] M. Muschol, F. Rosenberger, Interactions in undersaturated and supersaturated lysozyme solutions: static and dynamic light scattering results, J. Chem. Phys. 103 (1995) 10424–10432.
[2] M. Muschol, F. Rosenberger, Lack of evidence for prenucleation aggregate formation in lysozyme crystal growth solutions, J. Cryst. Growth 167 (1996) 738–747.
[3] R.F. Xiao, D.J.I. Alexander, F. Rosenberger, The morphological evolution of a growing crystal, Phys. Rev., A 38 (1988) 2447–2456.
[4] D.J.I. Alexander, in: J.P. van der Eerden, O.S.L. Bruinsma (Eds.), Science and Technology of Crystal Growth, Lattice Models, Kluwer Academic Publishers, The Netherlands, 1995, pp. 81–95.
[5] S. Tanaka, M. Yamamoto, K. Kawashima, K. Ito, R. Hayagawa, M. Ataka, Kinetic study on the early stage of the crystallization process of two forms of lysozyme crystals by photon correlation spectroscopy, J. Cryst. Growth 168 (1996) 44–49.
[6] S. Tanaka, M. Yamamoto, K. Ito, R. Hayagawa, M. Ataka, Relation between the phase separation and the crystallization in protein solutions, Phys. Rev., E 56 (1997) R67–R69.
[7] W. Eberstein, Y. Georgalis, W. Saenger, Molecular interactions in crystallizing lysozyme solutions studied by photon correlation spectroscopy, J. Cryst. Growth 143 (1994) 71–78.
[8] Y. Georgalis, P. Umbach, D.M. Soumpasis, W. Saenger, Ordering of fractal nuclei in crystallizing lysozyme solutions, J. Am. Chem. Soc. 121 (1999) 1627–1635.
[9] J.B. Bishop, W.J. Fredericks, S.B. Howard, T. Sawada, Dynamic light scattering analysis of solutions from which lysozyme crystals grow, J. Cryst. Growth 122 (1992) 41–49.
[10] M. Niimura, Y. Minezaki, M. Ataka, T. Katsura, Aggregation in supersaturated lysozyme solution studied by time-resolved small angle neutron scattering, J. Cryst. Growth 154 (1995) 136–144.
[11] M. Niimura, M. Ataka, Y. Minezaki, T. Katsura, Small angle neutron scattering from lysozyme crystallization process, Physica, B 213–214 (1995) 745.
[12] W.S. Price, F. Tsuchiya, Y. Arata, Time dependence of aggregation in crystallizing lysozyme solutions probed using NMR self-diffusion measurements, Bipophys. J. 80 (2001) 1585–1590.
[13] J. Poznański, J. Szymański, T. Basinska, S. Słomkowski, W. Zielenkiewicz, Aggregation of aqueous lysozyme solutions followed by dynamic light scattering and ^{1}H NMR spectroscopy, J. Mol. Liq, accepted.
[14] A. George, W.W. Wilson, Predicting protein crystallization from a dilute solution property, Acta Crystallogr., D Biol. Crystallogr. 50 (1994) 361–365.
[15] P.R. ten Wolde, D. Frenkel, Enhancement of protein crystal nucleation by critical density fluctuations, Science 277 (1997) 1975–1978.
[16] D. Rosenbaum, P.C. Zamora, C.F. Zukoski, Phase behavior of small attractive colloidal particles, Phys. Rev. Lett. 76 (1996) 150–153.
[17] W.C.K. Poon, Crystallization of globular proteins, Phys. Rev., E 55 (1997) 3762–3764.
[18] Y. Georgalis, P. Umbach, A. Zielenkiewicz, E. Utzig, W. Zielenkiewicz, P. Zielenkiewicz, W. Saenger, Microcalorimetric and small-angle light scattering studies on nucleating lysozyme solutions, J. Am. Chem. Soc. 119 (1997) 11959.
[19] M.A. Walsh, T.R. Schneider, L.C. Sieker, Z. Dauter, V.S. Lamzin, K.S. Wilson, Refinement of triclinic hen egg-white lysozyme at atomic resolution, Acta Crystallogr. D54 (1998) 522–546.
[20] L.K. Steinrauf, Structures of monoclinic lysozyme iodide at 1.6Å and of triclinic lysozyme nitrate at 1.1Å, Acta Crystallogr., D Biol. Crystallogr. 54 (1998) 767–779.
[21] H. Oki, Y. Matsuura, H. Komatsu, A.A. Chernov, Refined structure of orthorhombic lysozyme crystallized at high temperature: correlation between morphology and intermolecular contacts, Acta Crystallogr., D Biol. Crystallogr. 55 (1999) 114–121.
[22] M.C. Vaney, I. Broutin, P. Retailleau, A. Douangamath, S. Lafont, C. Hamiaux, T. Prangé, A. Ducruix, M. Riès-Kautt, Structural effects of monovalent anions on polymorphic lysozyme crystals, Acta Crystallogr., D Biol. Crystallogr. 57 (2001) 929–940.
[23] K. Lim, A. Nadarajah, E.L. Forsythe, M.L. Pusey, Locations of bromide ions in tetragonal lysozyme crystals, Acta Crystallogr., D Biol. Crystallogr. 54 (1998) 899–904.
[24] Z. Dauter, M. Dauter, Anomalous signal of solvent bromides used for phasing of lysozyme, J. Mol. Biol. 289 (1999) 93–101.
[25] C. Sauter, F. Otálora, J.A. Gavira, O. Vidal, R. Giegé, J.M. García-Ruiz, Structure of tetragonal hen egg-white lysozyme at 0.94 Å from crystals grown by the counter-diffusion method, Acta Crystallogr., D Biol. Crystallogr. 57 (Pt 8) (2001) 1119–1126.
[26] L. Sibille, M.L. Pusey, Investigation of nucleating lysozyme solutions, Acta Crystallogr., D Biol. Crystallogr. 50 (1994) 396–397.
[27] Z. Dauter, M. Dauter, K.R. Rajashankar, Novel approach to phasing proteins: derivatization by short cryo-soaking with halides, Acta Crystallogr., D Biol. Crystallogr. 56 (2000) 232–237.
[28] D.W. Marquardt, An algorithm for least-squares estimation of non-linear parameters, J. Soc. Ind. Appl. Math. 11 (1963) 431–441.
[29] T. Williams, C. Kelley, Gnuplot version 3.7, Copyright © (1998).
[30] W.G. McMillan, J.E. Mayer, Statistical thermodynamics of multi-component systems, J. Chem. Phys. 13 (1945) 276–305.
[31] F. Franks, M.D. Pedley, D.S. Reid, Solute interactions in dilute aqueous solutions: Part 1. Microcalorimetric study of the hydrophobic interaction, J. Chem. Soc., Faraday Trans. 1 (72) (1976) 359–367.
[32] S. Brandt, Data analysis, Statistical and Computational Methods for Scientists and Engineers with Extensive Source Program Libraries in FORTRAN, 3rd ed., Springer, New York, 1999.
[33] M. Wszelaka-Rylik, Determination of lysozyme enthalpic pairwise interaction parameters using a titration calorimeter at 288.15, 298.15 and 308.15 K, Bull. PAS Chem. 51 (2003) 135–141.
[34] A. Ben-Naim, Statistical mechanical study of hydrophobic interaction: II. Interaction among a set of M identical, spherical, and nonpolar solute particles, J. Chem. Phys. 54 (1971) 3696–3711.
[35] J. Poznański, M. Wszelaka-Rylik, W. Zielenkiewicz, Concentration dependencies of NaCl salting of lysozyme by calorimetric methods, Thermochim. Acta 409 (2004) 25–32.
[36] P. Umbach, Y. Georgalis, W. Saenger, Time-resolved small-angle static light scattering on lysozyme during nucleation and growth, J. Am. Chem. Soc. 120 (1998) 2382–2390.
[37] Y. Georgalis, P. Umbach, J. Raptis, W. Saenger, Lysozyme aggregation studied by light scattering: I. Influence of concentration and nature of electrolytes, Acta Crystallogr., D Biol. Crystallogr. 53 (1997) 691–702.